Surface Science 643 (2016) 203–209

Contents lists available at ScienceDirect

Surface Science

journal homepage: www.elsevier.com/locate/susc

Resolubility of image-potential resonances

Ulrich Höfer [a,b,*], Pedro M. Echenique [b,c]

[a] Fachbereich Physik und Zentrum für Materialwissenschaften, Philipps-Universität, 35032 Marburg, Germany
[b] Donostia International Physics Center (DIPC), 20018 San Sebastián, Spain
[c] Departamento de Física de Materiales, UPV/EHU and CFM-MPC, Centro Mixto CSIC-UPV/EHU, San Sebastián, Spain

ARTICLE INFO

Available online 23 July 2015

Keywords:
Image-potential state
Surface resonance
Open quantum system

ABSTRACT

A theory of image-potential states is presented for the general case where these surface electronic states are resonant with a bulk continuum. The theory extends the multiple scattering approach of Echenique and Pendry into the strong coupling regime while retaining independence from specific forms of surface and bulk potentials. The theory predicts the existence of a well-resolved series of resonances for arbitrary coupling strengths. Surprisingly, distinct image-potential resonances are thus expected to exist on almost any metal surface, even in the limiting case of jellium.

1. Introduction

At surfaces and interfaces of metals, atomic, molecular or other discrete electronic levels couple to a continuum of states in the volume. The accurate physical description of this coupling is central to understanding a wide variety of basic processes in catalysis, nanoscience or molecular electronics. Here, we consider one of the most simple, yet fundamental model systems of this kind, image-potential states, resonant with a structureless continuum.

Experimental and theoretical studies of the ultrafast dynamics of electrons in image-potential states have vastly improved our understanding of electronic excitation and decay processes at surfaces of metals [1]. Electrons excited to these states experience the Coulombic image force perpendicular to the metal surface. For crystallographic faces which exhibit a gap of the projected bulk bands in the vicinity of the vacuum energy, this gives rise to a Rydberg series of states, characterized by hydrogen-like wavefunctions in the vacuum and exponentially decaying Bloch waves in the bulk [2,3]. The conceptual simplicity of these electronic states and their well-defined properties have not only allowed to identify and quantify the important factors that govern their decay [4,5]. In fact, they have attained the role of a kind of drosophila of electron dynamics. As such, they serve as a benchmark system for the development of new ultrafast experimental techniques and as a reference for investigations of more complex electron transfer processes [6–15].

Recently, several experiments showed the existence of a well-defined series of similar states in the absence of a projected band gap [14,16,17]. Such image-potential resonances are depopulated mainly by elastic electron transfer into the bulk whereas the classical image-potential states can only decay inelastically. Since resonant elastic channels are expected to dominate electron transfer processes at interfaces in most applications, model studies of the decay of image-potential resonances are most interesting. These perspectives are, however, seriously hampered by the lack of a rigorous theoretical description which goes beyond appropriately tuned model potentials [18,19]. The multiple scattering theory of Echenique and Pendry [2] to free-electron-like metals as well as density functional theory at the level of the GW approximation predict just one broad resonance [20,21]. These results, which had been well accepted for many years, are now contradicted by recent experiments for Al(100) [16].

In this paper, we extend the theory of Ref. [2] in order to allow all scattering channels to interfere. It will be shown that such interference effects decisively change the solution in the regime of strong coupling leading to the full resolubility of the Rydberg series beyond the $n = 1$ state.

2. Theoretical model

We follow ideas first introduced by Feshbach for problems in nuclear physics [22] and apply an *open* quantum system formalism. In this approach one considers the following non-Hermitian effective Hamiltonian

$$\mathcal{H}_{\text{eff}} = \mathcal{H}_0 - iVV^{\dagger}. \tag{1}$$

$\mathcal{H}_0$ describes the unperturbed states. In practice, it is an $N \times N$ matrix with diagonal elements E_n and all off-diagonal elements equal to zero (no configuration interaction). V is a $K \times N$ matrix that describes the coupling to K continuum channels. The eigenvalues λ of $\mathcal{H}_{\text{eff}}$ are complex, with $E_{\text{res}} = \text{Re}(\lambda)$ denoting the maxima of the density of states and $\Gamma_{\text{res}} = -2\text{Im}(\lambda)$ their widths.

This type of *open* quantum system formalism has successfully been used to solve problems in various fields of physics [23,24]. Gauyacq and

* Corresponding author.
E-mail address: hoefer@physik.uni-marburg.de (U. Höfer).

http://dx.doi.org/10.1016/j.susc.2015.07.019
0039-6028/

co-workers have applied it to interpret results they obtained for the interaction of two atomic helium levels as a function of the distance from an aluminum surface [25] and, more recently, to explain the long excited-state lifetime of a metallic double chain adsorbed on Cu(111) [26].

Before we apply the formalisms to the series of image-potential resonances, it is instructive to simply consider two levels coupled to one continuum channel,

$$\mathcal{H}_{\text{eff}} = \begin{pmatrix} -\frac{E_0}{2} & \\ & +\frac{E_0}{2} \end{pmatrix} - i\alpha \begin{pmatrix} 1 & \sqrt{f} \\ \sqrt{f} & f \end{pmatrix}. \tag{2}$$

Without loss of generality the two levels are assumed to have energies $\mp E_0/2$, the lower one with stronger coupling and the upper one with a coupling that is smaller by a factor of f. The parameter α is a measure of the overall coupling strength of both levels to the continuum.

One notices that the coupling matrix $iVV^{\dagger}$ in $\mathcal{H}_{\text{eff}}$ (2) does not only contain the diagonal elements $i\alpha$ and $i\alpha f$ describing a decay. It also contains the off-diagonal coupling terms $i\alpha\sqrt{f}$. As shown explicitly in Appendix A, the resulting interference is mediated by the continuum. In the coupled system, not only the two levels are affected by the continuum. Similarly, the initially structureless continuum is disturbed upon interaction with the two levels and this disturbance, in turn, acts back on the resonances. Although $\mathcal{H}_{\text{eff}}$ does not describe the continuum itself, it includes this interference effect in leading order.

The complex eigenvalues of Eq. (2) are

$$\lambda_{1,2} = \mp\frac{1}{2}\sqrt{E_0^2 - \alpha^2(1+f)^2 + i2\alpha E_0(1-f)} - i\alpha\frac{1+f}{2}. \tag{3}$$

The dependence of this solution on the value of the coupling parameters α and f is illustrated in Fig. 1. One recognizes that the two resonances attract each other with increasing coupling strengths α. Whereas the width of the lower, more strongly coupled resonance Γ_1 increases monotonously with α, the width Γ_2 of the more weakly coupled upper resonance attains a maximum width around $\alpha(1+f) = 1$. For this coupling, the combined half width of both resonances $\Gamma_{\text{tot}}/2 = \alpha(1+f)$ equals the initial level spacing E_0. In the limit of large coupling, the lower resonance attains the total width $\alpha(1+f)$ whereas the other one becomes infinitely sharp (see Appendix A). This narrowing is known as resonance trapping [23].

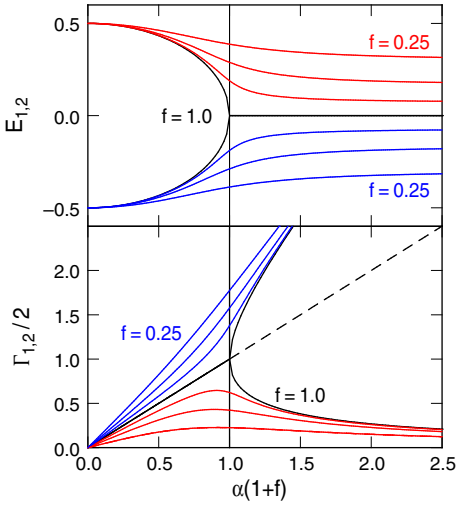

Fig. 1. Energy positions $E_i = \text{Re}(\lambda_i)$ and half widths $\Gamma_i/2 = -\text{Im}(\lambda_i)$ of the two-level system (2, 3) as a function of the total coupling strength $\alpha(1+f)$ for $E_0 = 1$ and $f = \frac{1}{4}, \frac{1}{2}, \frac{3}{4}, 1$. The dashed line denotes $\Gamma_{\text{tot}}/2 = \alpha(1+f)$. In the special case $f = 1$ both resonances are centered at $E = 0$ for $\alpha(1+f) \geq 1$.

The construction of the effective Hamiltonian (1) for the series of image-potential resonances requires the energy levels of the decoupled series and the coupling strengths to the metallic continuum. These values are obtained from the multiple scattering theory [2]. Within this approach a surface state is viewed as a wave trapped between the bulk crystal and the surface barrier, similar to the modes of a Fabry–Pérot interferometer. The repeated scattering at the crystal boundary and the surface barrier results in an amplitude

$$\frac{1}{1 - r_B r_C \exp i(\phi_B + \phi_C)} \tag{4}$$

where ϕ_B and ϕ_C denote the phase changes between incident and reflected waves at the surface barrier and at the crystal, respectively. r_B and r_C are the corresponding reflectivities. In the usual image-state problem $r_B = r_C = 1$ and the condition for bound states is

$$\phi_B + \phi_C = 2\pi n, \quad n = 0, 1, 2, \ldots \tag{5}$$

In the case of resonances, the loss of flux due to elastic electron transfer to bulk states results in $r_C < 1$. This can be accounted for in terms of a complex phase $\phi_C = \phi_C' + i\phi_C''$ with an imaginary component $\phi_C'' = -\ln r_C$ [2].

Since this scattering model does not take a possible perturbation of the continuum by the resonances into account, a direct evaluation of Eq. (4) will not yield the proper energies and widths of the resonances when r_C is small, i.e., in the case of strong coupling. In the weak coupling limit ($r_C \to 1$), however, it can safely be employed to determine energies and *relative* coupling strengths, the only input needed to construct $\mathcal{H}_{\text{eff}}$. In linear approximation, the condition (5) is fulfilled for

$$\frac{\Gamma}{2}\frac{\partial}{\partial E}(\phi_B + \phi_C') = \phi_C'' \tag{6}$$

with $\Gamma/2$ being the energy dependent decay rate of the amplitude (4).

For the energy dependence of the phase change ϕ_B at the image potential we use the WKB approximation [27], $\phi_B \simeq [(-8E)^{-1/2} - 1]\pi$. Above the band gap $\phi_C' = \pi$ (see below), and we obtain a Rydberg series of resonances

$$E_n^0 = -\frac{1}{32n^2}, \quad n = 1, 2, \ldots \tag{7}$$

with a decay rate or full width at half maximum given by

$$\Gamma_n^0 = \frac{-\ln r_C\left(E_n^0\right)}{2\pi}\frac{1}{8n^3}, \quad n = 1, 2, \ldots \tag{8}$$

In the case of a simple metal it is sufficient to restrict oneself to one continuum ($K = 1$) like in the above example of the two-level system. Since Eq. (8) must correspond to the solution of Eq. (1) in the limit of small coupling, the matrix elements V_n are determined by the condition $|V_n|^2 = \Gamma_n^0/2$.

In addition to a n^3-dependence, the Γ_n^0 depends weakly on the quantum number n via the energy dependence of the reflectivity r_C. In order to facilitate a general discussion, we will neglect this weak dependence in the following. This approximation allows us to introduce the dimensionless parameter

$$\alpha = \frac{1}{\pi}(-\ln r_C) \tag{9}$$

as a measure of the overall resonant coupling strength of the whole series and we obtain

$$|V_n|^2 = \frac{\Gamma_n^0}{2} = \frac{\alpha}{32n^3}. \tag{10}$$

Please note that in terms of the numerical matrix diagonalization necessary to find the complex eigenvalues of Eq. (1), the approximation of a constant r_C has no advantage and can easily be dropped in calculations for specific materials. However, it will become apparent below that for the most interesting cases of strong coupling the energy dependence of r_C is indeed negligible over the limited range of energies E_n^0.

The resulting energies and widths of the first five resonances are plotted in Figs. 2 and 3 as function of the coupling parameter α. Specific numerical values of interest are collected in Table 1. In the limiting case $r_C \to 1$ or $\alpha \to 0$ the eigenvalues of Eq. (1) evidently give exactly the resonance spectrum (7) and (8). As expected from the above analysis of the two-level system, dramatic changes occur as soon as $\Gamma_n^0/2 + \Gamma_{n+1}^0/2 \simeq \Gamma_n^0 = \alpha/16n^3$ starts to approach the level spacing $\Delta_n^0 = E_{n+1}^0 - E_n^0 \simeq 1/16n^3$, i.e., when α approaches unity [28].

In the regime of small coupling ($\alpha \lesssim 0.2$) all resonances develop uniformly and simply broaden linearly as a function of α (Fig. 3). With increasing coupling the behavior of the $n = 1$ resonance and the other resonances become qualitatively different. Whereas the width of $n = 1$ increases monotonically and spreads over the whole spectrum for $\alpha \gtrsim 0.5$, all other resonances reach a maximum width Γ_n^{max} and get narrower again for further increasing α. The higher the quantum number n, the sooner Γ_n^{max} is reached (Fig. 2). The positions of the resonances also change as a function of coupling strength until they reach a limiting value E_n^∞ for large α. As illustrated by Fig. 3, the first resonance and the series of all other resonances effectively attract each other with increasing coupling. This attraction is larger, the lower the quantum number n. As a result, the resonances $n = 2, 3, \ldots$ spread as a function of α. For the maximum coupling strength $\alpha = 1$ plotted in Fig. 3, the energies E_n have reached their limiting values already within 2% whereas the deviation from the uncoupled situation is more than 30% for $n = 2$.

Most importantly, if one compares the widths and the energy separation of the resonances $n = 2, 3, \ldots$ (Fig. 3), they are found to be well separated throughout the range of coupling strengths $\alpha = 0 \to \infty$. Even around $\alpha = 0.5$ where they reach their maximum widths Γ_n^{max}, the combined half-width of neighboring resonances stays well below their energy difference. *This means – with the notable exception of the first resonance – that the integrity of the Rydberg series is not destroyed by strong coupling to a continuum.* In contrast, stronger coupling even leads to a sharper spectrum of the higher resonances as compared to intermediate coupling.

This, at first glance, surprising result is understood in a straightforward manner by considering the effective Hamiltonian (1) in the limit $\alpha \to \infty$. In that case the matrix $VV^\dagger$ determines the behavior of the system and one expects to obtain K states that take almost the whole coupling and $N - K$ states that are almost decoupled. For our case of one continuum ($K = 1$), the most strongly coupled resonance ($n = 1$) becomes the fast (open) channel with $\Gamma_1/2 \sim -\mathrm{Im}\{Tr(\mathcal{H}_{\mathrm{eff}})\}$ whereas $n = 2, 3, \ldots$ become long lived (trapped) states. A reorganization of the system due to interference of the different decay channel takes place already for intermediate values of α. As a consequence, the resonance spectrum never gets totally smeared out as one might intuitively expect.

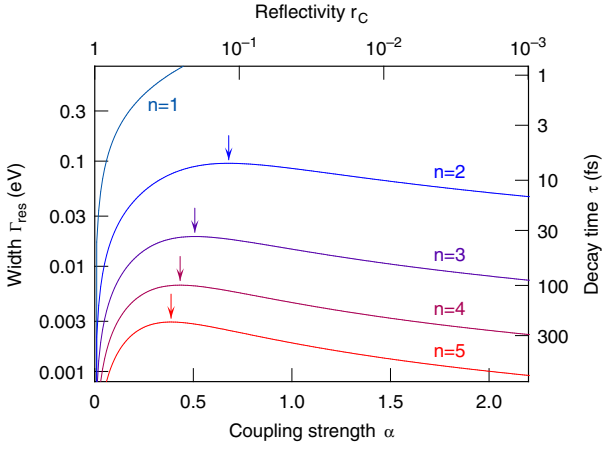

Fig. 2. Half widths and decay times of the first five resonances as a function of coupling strength and reflectivity. Arrows indicate coupling strengths where maximum widths are reached.

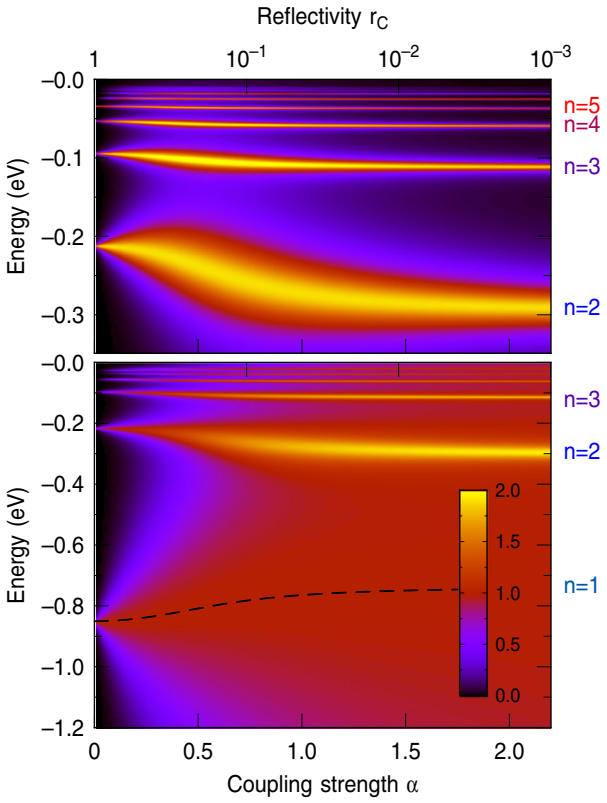

Fig. 3. (a) False color contour plot of resonance spectra $n = 1, \ldots, 5$ as a function of coupling strength/reflectivity. For better visibility the Lorentzians of the individual resonances are superimposed with equal amplitudes (not areas); the dashed line indicates the maximum of $n = 1$ resonance. (b) Resonance spectra $n = 2, \ldots, 5$ on an expanded scale; the transition between red and blue colors occurs approximately at half the maximum amplitude.

In terms of the basic physical processes, the trapping is nothing else than a back feeding of intensity from the distorted continuum into the more weakly coupled states. This is easily recognized in the example of the two level system discussed in the appendix. If the system in state $|a\rangle$ is coupled to the continuum at $t = 0$, the amplitude $a(t)$ will start to decay. At the same time, the amplitude $b(t)$, which was initially equal to zero, will start to increase in reaction to the distortion of the continuum (Eq. A1). Since the amplitude $b(t)$ has the opposite phase as $a(t)$, the coupling of state $|b\rangle$ to the continuum will in turn accelerate the decay of state $|a\rangle$.

Table 1
Limiting values of energies E_n^0, $E_n^\infty \equiv E_n(\alpha \to \infty)$, maximum widths Γ_n^{max}, minimum lifetimes τ_n^{min} and corresponding coupling parameter $\alpha(\Gamma_n^{max})$ for the first five resonances.

	E_n^0 (eV)	E_n^∞ (eV)	Γ_n^{max} (eV)	τ_n^{min} (fs)	$\alpha(\Gamma_n^{max})$
$n = 1$	−0.8504	−0.7363	–	–	–
$n = 2$	−0.2126	−0.2967	0.09545	6.90	0.6795
$n = 3$	−0.0945	−0.1221	0.01920	34.28	0.5076
$n = 4$	−0.0531	−0.0593	0.00662	99.43	0.4329
$n = 5$	−0.0340	−0.0368	0.00295	223.10	0.3871

3. Results of Ag(111), Al(100) and Al(111)

In our description, the only material-dependent parameter is the reflectivity r_C of a free electron wave at the surface. For surfaces of simple metals, like Ag(100), Al(100) and Al(111), it can simply be obtained from the two-band model of the bulk electronic structure [29]. For a distance a of lattice planes along the surface normal and an *sp*-gap at the $\bar{\Gamma}$ – point of $2V_g$, the potential of the two-band model is

$$V(z) = -V_0 + V_g e^{igz} + V_g e^{-igz} \tag{11}$$

with $g = 2\pi/a$, and V_0 chosen such that the vacuum level is at zero energy. We restrict ourselves to a situation where the image-potential states are resonant with the upper band

$$E(k) = -V_0 + \left(\frac{g}{2}\right)^2 + k^2 + \sqrt{V_g^2 + g^2k^2}. \tag{12}$$

The wave functions that solve the Schrödinger equation are Bloch waves in the crystal ($z < 0$) and plane waves in the vacuum ($z > 0$)

$$\Psi_C = \alpha e^{i\left(\frac{g}{2}-k\right)z} + \beta e^{-i\left(\frac{g}{2}+k\right)z}, \quad z \le 0 \tag{13a}$$

$$\Psi_{vac} = Ae^{iqz} + Be^{-iqz}, \quad z \ge 0 \tag{13b}$$

with wave vectors

$$k = \sqrt{E + V_0 + \left(\frac{g}{2}\right)^2 - \sqrt{(E+V_0)g^2 + V_g^2}}$$

$$q = \sqrt{E + V_0}.$$

The reflectivity r_C is the ratio A/B of the in- and outgoing plane wave Ψ_{vac} in the vacuum, obtained from matching conditions at the interface $(\Psi_C'/\Psi_C|_{z=0} = \Psi_{vac}'/\Psi_{vac}|_{z=0})$ [30]:

$$r_C = \frac{A}{B} = \frac{V_g\left(q-k+\frac{g}{2}\right) + V'\left(q-k-\frac{g}{2}\right)}{V_g\left(q+k-\frac{g}{2}\right) + V'\left(q+k+\frac{g}{2}\right)} \tag{15}$$

with

$$V' = V_g\frac{\beta}{\alpha} = gk + \sqrt{V_g^2 + g^2k^2}.$$

Parameters used to describe the three surfaces Ag(111), Al(100), and Al(111) and the resulting reflectivities r_C and coupling parameters $\alpha = -\pi^{-1}\ln r_C$ for $E = E_{vac} \equiv 0$ are collected in Table 2. Explicit values of the calculated resonance energies and lifetimes are given in Table 3. r_C is equal to one at the edge of the upper band ($k = 0$) and decreases monotonously as the energy increases. This decrease is more rapid, the smaller the value of V_g (Fig. 4).

Table 2
Reflectivities at the vacuum energy $r_C(E = 0)$ and coupling strengths α for Ag(111), Al(100) and Al(111); parameters have been derived from the values given in Ref. [31] (band gap: $E_{gap} = 2V_g$, upper band edge: $E_{up} = E(k = 0)$).

Surface	a (°A)	V_g (eV)	V_0 (eV)	E_{up} (eV)	r_C	α
Ag(111)	$4.085/\sqrt{3}$	2.150	9.3619	−0.4527	0.51	0.22
Al(100)	$4.049/\sqrt{2}$	0.840	10.9723	−5.5450	0.054	0.92
Al(111)	$4.049/\sqrt{3}$	0.125	15.6485	−8.6425	0.0059	1.63

Table 3
Energies E_n and decay times τ_n of the first seven image-potential resonances of Ag(111), Al(100) and Al(111).

	Ag(111)		Al(100)		Al(111)	
	E_n (eV)	τ_n (fs)	E_n (eV)	τ_n (fs)	E_n (eV)	τ_n (fs)
$n = 1$	–	–	−0.767	0.4	−0.745	0.2
$n = 2$	−0.211	16.2	−0.270	7.3	−0.288	10.8
$n = 3$	−0.095	49.6	−0.109	41.6	−0.111	65.9
$n = 4$	−0.054	116.2	−0.058	130.7	−0.059	221.4
$n = 5$	−0.034	229.2	−0.037	307.3	−0.037	502.9
$n = 6$	−0.024	402.6	−0.025	608.6	−0.025	1003.6
$n = 7$	−0.018	651.0	−0.018	1075.2	−0.018	1782.9

Experimental data for the series of image-potential resonances are available for Ag(111) [17] and Al(100) [16]. Fig. 5 shows that the present theory is able to describe the measured lifetimes within a factor of two. Apparently, the two-band model predicts somewhat too small values of r_C. In the case of Ag(111), this results in shorter lifetimes than the experimental ones. In the case of Al(100), on the contrary, too small values of r_C overestimate the lifetimes of the high-n states that are already effectively trapped.

For Ag(111) $n = 1$ is still a gap state, r_C is 50% near the vacuum energy. The corresponding coupling parameter is $\alpha = 0.22$. Trapping will thus be effective only for resonances with higher quantum numbers. For Al(100) the reflectivity is only 5% and the coupling parameter is $\alpha = 0.92$. The theory predicts a very broad first resonance and widths of the high-n resonances that are substantially reduced as compared to the model of independent decay. The quantitative comparison with the experimental data of Refs. [17] and [16] shows good quantitative agreement for both surfaces, particularly if one considers that we neglect other decay channels and make use of the most simple estimate for r_C. Al(111) is a surface very close to the idealized jellium model with a very low electron reflectivity ($r_C = 0.6\,\%$). With a resulting coupling parameter $\alpha = 1.63$ the present theory predicts high-n resonances that are sharper and more long-lived than those of Al(100) and even those of Ag(111). Electrons in these resonances are effectively trapped (Fig. 2).

It must be pointed out that the result for Al(111) stands in marked contradiction with some of the established knowledge from the literature. Previous experimental and theoretical work agree on the presence of just one structureless feature near the vacuum level for Al(111) arising from image-potential resonances [32–35,20,21]. The same holds for the icosahedral Al-Pd-Mn quasicrystal [36]. However, the experimental resolution of Refs. [32–34,36] did not exceed 200 meV and was thus not sufficient to resolve high-n resonances. A reinvestigation of well-defined Al(111) with improved experimental possibilities would therefore be highly desirable. The Al(111) surface would also provide interesting opportunities to decouple the resonances by adlayers. The present theory clearly predicts that moderate decoupling should lead to shorter lifetimes of the high-n resonances, and not to longer ones as for image-potential states at gaps [37].

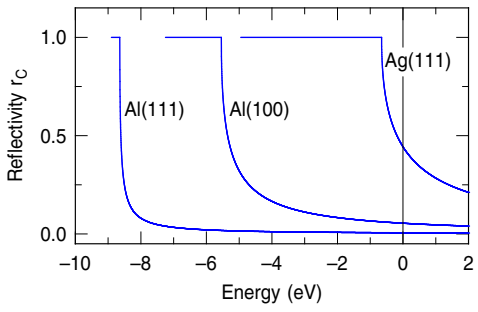

Fig. 4. Energy dependence of the reflectivity r_C for Al(111), Al(100), and Ag(111) as calculated from the two-band model.

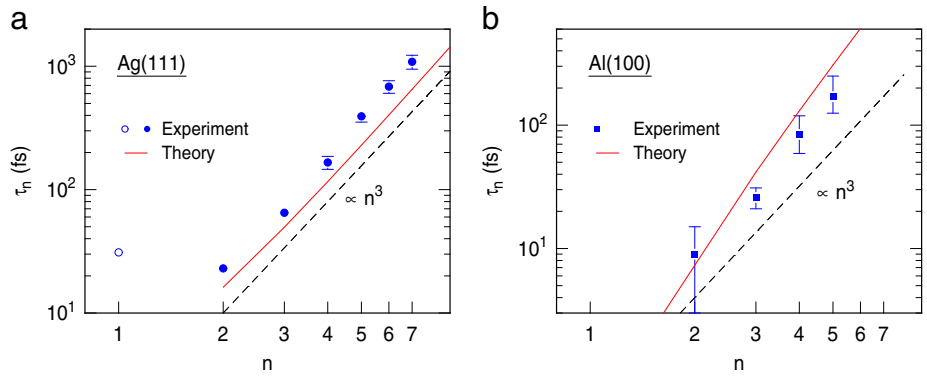

Fig. 5. Comparison of measured lifetimes (full circles) with calculated values (solid line) using reflectivities r_C from the two-band model (Table 2) for Ag(111) (a) and Al(100) (b); a common coupling parameter of $\alpha = 0.92$ was used for Al(100), whereas the energy dependence of r_C was taken into account for Ag(111). For this surface, $n = 1$ (open circle) is an inelastically decaying gap state [17].

4. Conclusions

In conclusion, we have shown that electrons in energetically adjacent states, strongly coupled to a continuum at a metal interface, do not delocalize independently from each other. Interference effects can lead to extremely long lifetimes of some states while others experience an accelerated decay. Criterium for strong coupling is a significant overlap of the broadened levels, not the absolute coupling strength. One expects it to be fulfilled in a variety of situations in nanoscience, catalysis or molecular electronics, e.g., when small clusters or organic molecules with many close lying levels interact with a substrate. As for the Rydberg series of image-potential resonances, our theory strengthens the prediction of Echenique and Pendry [2], who stated that the whole series of states would be observable whenever the first two ones are separated. With the notable exception of the first resonance, a series of clearly separated resonances should exist for all coupling strengths, i.e., on any well-defined metal surface.

Acknowledgment

We thank J.-P. Gauyacq, T.F. Heinz, P. Thomas and M. Winter for the valuable discussions and acknowledge funding by the Deutsche Forschungsgemeinschaft through SFB 1083.

Appendix A. Effective Hamiltonian of the two-level system

In the literature, the effective Hamilton operator $\mathcal{H}_{\text{eff}}$ for the general case of n levels interacting with several continua is usually obtained by means of the Feshbach projection operator formalism [22,24,38]. Much of the essential physics, however, is already revealed by considering two levels coupled to one structureless continuum [39]. In the following we give a simple derivation of $\mathcal{H}_{\text{eff}}$ for the two-level system (2) and evaluate its properties. In this way, we hope to make the approach more easily accessible to the general surface science reader.

The Hamilton operator of two electronic states $|a\rangle$ and $|b\rangle$ with energies E_a and E_b coupled to a continuum by an interaction V is

$$H = H_0 + V = E_a|a\rangle\langle a| + E_b|b\rangle\langle b| + \sum_\mu \omega_\mu|\mu\rangle\langle\mu| + V.$$

We consider here only an interaction between the states $|a\rangle$ and $|b\rangle$ and the continuum states $|\mu\rangle$

$$\langle a|V|\mu\rangle = V_a, \quad \langle b|V|\mu\rangle = V_b.$$

This interaction is assumed to be energy independent; all other matrix elements $\langle|V|\rangle$ vanish. The time dependence of the wave function of the full system

$$|\Psi(t)\rangle = a(t)|a\rangle + b(t)|b\rangle + \sum_\mu \hat{c}_\mu(t)e^{-i\omega_\mu t}|\mu\rangle$$

is determined by the Schrödinger equation $H|\Psi\rangle = i\partial_t|\Psi\rangle$ which reads in matrix form

$$i\partial_t\begin{pmatrix} a \\ b \\ \hat{c}_1 e^{-i\omega_1 t} \\ \vdots \\ \hat{c}_N e^{-i\omega_N t}\end{pmatrix} = \begin{pmatrix} E_a & & V_a & \cdots & V_a \\ & E_b & V_b & \cdots & V_b \\ V_a & V_b & \omega_1 & & \\ \vdots & \vdots & & \ddots & \\ V_a & V_b & & & \omega_N \end{pmatrix}\begin{pmatrix} a \\ b \\ \hat{c}_1 e^{-i\omega_1 t} \\ \vdots \\ \hat{c}_N e^{-i\omega_N t}\end{pmatrix}$$

or as a set of coupled differential equations

$$i\partial_t a(t) = E_a a(t) + V_a\sum_\mu \hat{c}_\mu(t)e^{-i\omega_\mu t} \tag{A1a}$$

$$i\partial_t b(t) = E_b b(t) + V_b\sum_\mu \hat{c}_\mu(t)e^{-i\omega_\mu t} \tag{A1b}$$

$$i\partial_t\left[\hat{c}_\mu(t)e^{-i\omega_\mu t}\right] = V_a a(t) + V_b b(t) + \omega_\mu\hat{c}_\mu(t)e^{-i\omega_\mu t}. \tag{A1c}$$

We are only interested in the time dependence of the states $|a\rangle$ and $|b\rangle$ due to their interaction with the continuum, not in the evolution of the continuum states themselves. We thus eliminate $\hat{c}_\mu$ from Eqs. (A1a) and (A1b) by integrating Eq. (A1c) and obtain

$$\hat{c}_\mu(t) = -i\int dt'\left[V_a a(t') + V_b b(t')\right]e^{i\omega_\mu t'}.$$

We further assume the continuum states $|\mu\rangle$ to be equally spaced and to extend from $-\infty$ to $+\infty$. Then the sums that appear in Eqs. (A1a) and (A1b) simply become

$$\begin{aligned}\sum_\mu \hat{c}_\mu(t)e^{-i\omega_\mu t} &= \int d\omega\, \hat{c}(\omega,t)e^{-i\omega t} \\ &= -i\int d\omega\int dt'\left[V_a a(t') + V_b b(t')\right]e^{i\omega(t'-t)} \\ &= -i2\pi\left[V_a a(t) + V_b b(t)\right]\end{aligned}$$

and we arrive at two coupled differential equations for the amplitudes $a(t)$ and $b(t)$

$$i\partial_t\begin{pmatrix} a(t) \\ b(t)\end{pmatrix} = \begin{pmatrix} E_a - i2\pi V_a^2 & -i2\pi V_a V_b \\ -i2\pi V_a V_b & E_b - i2\pi V_b^2\end{pmatrix}\begin{pmatrix} a(t) \\ b(t)\end{pmatrix}. \tag{A2}$$

We identify the matrix in Eq. (A2) with the effective Hamiltonian for the two-level system (2) with $E_{a,b} = \mp E_0/2$, $2\pi V_a^2 = \alpha$, and $2\pi V_b^2 = \alpha f$.

One recognizes that the coupling to the continuum not only introduces a finite width of the levels, given by $2\pi V_a^2 = \alpha$ and $2\pi V_b^2 = \alpha f$. In addition the two levels appear to interact with one another as described by the imaginary off-diagonal terms $i2\pi V_a V_b = i\alpha\sqrt{f}$. The derivation clearly reveals that this interaction is not a direct one, but one mediated by the continuum. The interaction with the levels $|a\rangle$ and $|b\rangle$ disturbs the continuum states $|\mu\rangle$. This time-dependent disturbance in turn acts back on $|a\rangle$ and $|b\rangle$. This interaction becomes stronger with a stronger coupling to the continuum, and it is directly linked to the level widths. The derivation also shows that the effective Hamiltonian (2) will be a good approximation for the full Hamiltonian as far as the levels are concerned, when the continuum is structureless and extends well beyond the energy spread of the broadened levels. This requirement is fulfilled in the case of the image-potential resonances considered in this work.

The effective Hamiltonian (2) of the two-level system with energies $\mp E_0/2$, overall coupling parameter α and relative coupling strength f ($0 < f \le 1$) has two complex eigenvalues

$$\lambda_{1,2} = \mp\frac{1}{2}\sqrt{E_0^2 - \alpha^2(1+f)^2 + i2\alpha E_0(1-f)} - i\alpha\frac{1+f}{2}. \qquad (3,\ \text{repeated})$$

The resulting resonance energies and widths can be written in the form

$$E_{1,2} = \mathrm{Re}\,\lambda_{1,2} = \mp\frac{1}{2}\rho\cos\frac{\varphi}{2} \qquad (A3a)$$

$$\Gamma_{1,2} = -2\,\mathrm{Im}\,\lambda_{1,2} = \alpha(1+f) \pm \rho\sin\frac{\varphi}{2} \qquad (A3b)$$

with $\rho = \rho(E_0, f, \alpha)$ and $\varphi = \varphi(E_0, f, \alpha)$. Obviously the total energy of the coupled system $E_{\mathrm{tot}} = E_1 + E_2 = 0$ does not change with the coupling parameter α while the total decay rate simply grows linearly with α

$$\Gamma_{\mathrm{tot}} = \Gamma_1 + \Gamma_2 = 2\alpha(1+f). \qquad (A4)$$

With increasing values of α, the energy separation of the two levels $\Delta = E_2 - E_1$ decreases. If one expands the solution into powers of α, one finds that the attraction is initially quadratic in α

$$\Delta(\alpha\to 0) = E_0 + \frac{f}{E_0}\alpha^2 - \ldots$$

and reaches a limiting value that depends on the relative coupling strength f

$$\Delta(\alpha\to\infty) = E_0\frac{1-f}{1+f} + \mathcal{O}\left(\frac{1}{\alpha^2}\right).$$

For the degenerate case $f = 1$ the attraction is strictly quadratic until the two levels coincide for $2\alpha \ge 1$. While the system remains completely symmetrical in terms of the energies of the two resonances, the initial asymmetry of the half widths is seen to increase as a function of α.

$$\frac{\Gamma_1}{2}(\alpha\to 0) = \alpha + \frac{\alpha^3}{E_0^2}f(1-f) + \ldots$$

$$\frac{\Gamma_2}{2}(\alpha\to 0) = f\alpha - \frac{\alpha^3}{E_0^2}f(1-f) + \ldots$$

The width Γ_1 of the more strongly coupled resonance increases monotonously. The width Γ_2, however, reaches a maximum value $\Gamma_{2,\max}$ and goes to zero in the limit of infinite coupling.

$$\frac{\Gamma_1}{2}(\alpha\to\infty) = (1+f)\alpha - \frac{E_0^2}{\alpha}\frac{f}{(1+f)^3} + \ldots$$

$$\frac{\Gamma_2}{2}(\alpha\to\infty) = \frac{E_0^2}{\alpha}\frac{f}{(1+f)^3} + \ldots$$

The maximum of Γ_2 is reached approximately when the real part of the argument under the square root in Eq. (3) becomes zero. This is the case for

$$\alpha_{\max}^0 = \frac{E_0}{1+f} \qquad (A5)$$

i.e., for a value where the total decay rate $\Gamma_{\mathrm{tot}}/2 = \alpha_{\max}^0(1+f)$ is equal to the initial level spacing E_0. For this coupling strength we have

$$\Delta(\alpha_{\max}^0) = E_0\sqrt{\frac{1-f}{1+f}} \qquad (A6a)$$

$$\Gamma_2(\alpha_{\max}^0) = E_0 - \Delta(\alpha_{\max}^0). \qquad (A6b)$$

These results concerning the maximum of Γ_2 are exact for $f = 1$. In this degenerate case, the widths of both levels increase strictly linear with α as long as $2\alpha \le 1$. For $2\alpha > 1$, when their energies coincide, one of them increases faster, while the other one decreases and approaches zero (see also Fig. 1 in the main text). For a ratio $f < 1$ Eq. (A5) slightly overestimates the coupling parameter a for which the maximum of Γ_2 is reached. The error, however, is less than 12% and less than 4% in expression (A6b) which slightly underestimates $\Gamma_{2,\max}$.

References

[1] U. Bovensiepen, H. Petek, M. Wolf (Eds.), "Dynamics at Solid State Surfaces and Interfaces: Volume 1 — Current Developments", Wiley-VCH, Weinheim, 2010.
[2] P.M. Echenique, J.B. Pendry, J. Phys. C 11 (1978) 2065.
[3] T. Fauster, W. Steinmann, in: P. Halevi (Ed.), Electromagnetic Waves: Recent Developments in Research, vol. 2 1995, p. 347 (North-Holland, Amsterdam).
[4] P.M. Echenique, R. Berndt, E.V. Chulkov, T.H. Fauster, A. Goldmann, U. Höfer, Surf. Sci. Rep. 52 (2004) 219.
[5] T. Fauster, M. Weinelt, U. Höfer, Prog. Surf. Sci. 82 (2007) 224.
[6] U. Höfer, I.L. Shumay, C. Reuß, U. Thomann, W. Wallauer, T. Fauster, Science 277 (1997) 1480.
[7] N.H. Ge, C.M. Wong, R.L. Lingle, J.D. McNeill, K.J. Gaffney, C.B. Harris, Science 279 (1998) 202.
[8] A.D. Miller, I. Bezel, K.J. Gaffney, S. Garrett-Roe, S.H. Liu, P. Szymanski, C.B. Harris, Science 297 (2002) 1163.
[9] K. Boger, M. Weinelt, T. Fauster, Phys. Rev. Lett. 92 (2004) 126803.
[10] J. Güdde, M. Rohleder, T. Meier, S.W. Koch, U. Höfer, Science 318 (2007) 1287.
[11] C.H. Schwalb, S. Sachs, M. Marks, A. Schöll, F. Reinert, E. Umbach, U. Höfer, Phys. Rev. Lett. 101 (2008) 146801.
[12] X.Y. Zhu, Q. Yang, M. Muntwiler, Acc. Chem. Res. 42 (2009) 1779.
[13] B. Borca, et al., Phys. Rev. Lett. 105 (2010) 036804.
[14] C. Eickhoff, M. Teichmann, M. Weinelt, Phys. Rev. Lett. 107 (2011) 176804.
[15] X.F. Cui, C. Wang, A. Argondizzo, S. Garrett-Roe, B. Gumhalter, H. Petek, Nat. Phys. 10 (2014) 505.
[16] M. Winter, E.V. Chulkov, U. Höfer, Phys. Rev. Lett. 107 (2011) 236801.
[17] M. Marks, K. Schubert, C.H. Schwalb, J. Güdde, U. Höfer, Phys. Rev. B 84 (2011) 245402.
[18] A.G. Borisov, E.V. Chulkov, P.M. Echenique, Phys. Rev. B 73 (2006) 073402.
[19] S.S. Tsirkin, A.G. Borisov, E.V. Chulkov, Phys. Rev. B 88 (2013) 035449.
[20] S. Papadia, M. Persson, L.A. Salmi, Phys. Rev. B 41 (1990) 10237.
[21] G. Fratesi, G.P. Brivio, P. Rinke, R.W. Godby, Phys. Rev. B 68 (2003) 195404.
[22] H. Feshbach, Ann. Phys. 5 (1958) 357.
[23] J. Okolowicz, M. Ploszajczak, I. Rotter, Phys. Rep. Rev. Sec. Phys. Lett. 374 (2003) 271.
[24] M. Desouter-Lecomte, V. Jacques, J. Phys. B Atomic Mol. Phys. 28 (1995) 3225.
[25] G.E. Makhmetov, A.G. Borisov, D. Teilletbilly, J.P. Gauyacq, Europhys. Lett. 27 (1994) 247.
[26] S. Diaz-Tendero, A.G. Borisov, J.-P. Gauyacq, Phys. Rev. Lett. 102 (2009) 166807.
[27] E.G. McRae, M.L. Kane, Surf. Sci. 108 (1981) 435.
[28] According to our definition, the dimensional parameter α corresponds exactly to the ratio Γ_n/Δ_n of the noninterfering system for large n.

[29] F. Schiller, A. Leonardo, E.V. Chulkov, P.M. Echenique, J.E. Ortega, Phys. Rev. B 79 (2009) 033410.
[30] The derived reflectivities are independent from a specific position of the boundary z_0 in the framework of this model.
[31] E.V. Chulkov, V.M. Silkin, P.M. Echenique, Surf. Sci. 437 (1999) 330.
[32] D. Heskett, K.H. Frank, E.E. Koch, H.J. Freund, Phys. Rev. B 36 (1987) 1276.
[33] S. Yang, R.A. Bartynski, G.P. Kochanski, S. Papadia, T. Fonden, M. Persson, Phys. Rev. Lett. 70 (1993) 849.
[34] V. Bulovic, B. Quiniou, R.M. Osgood, J. Vac. Sci. Technol. A 12 (1994) 2201.
[35] S.A. Lindgren, L. Wallden, Phys. Rev. B 40 (1989) 11546.
[36] M. Maniraj, Abhishek Rai, S.R. Barman, M. Krajci, D.L. Schlagel, T.A. Lograsso, K. Horn, Phys. Rev. B 90 (2014) 115407.
[37] J. Güdde, W. Berthold, U. Höfer, Chem. Rev. 106 (2006) 4261.
[38] I. Rotter, J. Phys. A Math. Theor. 42 (2009) 153001.
[39] A.Z. Devdariani, V.N. Ostrovskii, Y.N. Sebyakin, Sov. Phys. — JETP 44 (1976) 477.